



ELSEVIER

Original Article

# Synthesis, characterization, and evaluation of antimicrobial and cytotoxic effect of silver and titanium nanoparticles

Fidel Martinez-Gutierrez, MSc<sup>a</sup>, Peggy L. Olive, PhD<sup>b</sup>, Adriana Banuelos, PhD<sup>b</sup>, Erasmo Orrantia, PhD<sup>c</sup>, Nereyda Nino, PhD<sup>d</sup>, Elpidio Morales Sanchez, PhD<sup>e</sup>, Facundo Ruiz, PhD<sup>d</sup>, Horacio Bach, PhD<sup>f,\*</sup>, Yossef Av-Gay, PhD<sup>f</sup>

<sup>a</sup>Facultad de Ciencias Químicas, Universidad Autónoma de San Luis Potosí, San Luis Potosí, México

<sup>b</sup>British Columbia Research Centre, Vancouver, British Columbia, Canada

<sup>c</sup>Centro de Investigaciones de Materiales Avanzados, Chihuahua, México

<sup>d</sup>Facultad de Ciencias, Universidad Autónoma de San Luis Potosí, San Luis Potosí, México

<sup>e</sup>Departamento de Físico Matemáticas, Universidad Autónoma de San Luis Potosí, San Luis Potosí, México

<sup>f</sup>Department of Medicine, Division of Infectious Diseases, University of British Columbia, Vancouver, British Columbia, Canada

Received 28 October 2009; accepted 2 February 2010

## Abstract

Microbial resistance represents a challenge for the scientific community to develop new bioactive compounds. Nosocomial infections represent an enormous emerging problem, especially in patients with ambulatory treatment, which requires that they wear medical devices for an extended period of time. In this work, an evaluation of the antimicrobial activity of both silver and titanium nanoparticles was carried out against a panel of selected pathogenic and opportunistic microorganisms, some of them commonly associated with device-associated infections. Cytotoxicity assays monitoring DNA damage and cell viability were evaluated using human-derived monocyte cell lines. We show that silver-coated nanoparticles having a size of 20–25 nm were the most effective among all the nanoparticles assayed against the tested microorganisms. In addition, these nanoparticles showed no significant cytotoxicity, suggesting their use as antimicrobial additives in the process of fabrication of ambulatory and nonambulatory medical devices.

**From the Clinical Editor:** In this study, antimicrobial activity of silver and titanium nanoparticles was evaluated against a panel of selected pathogenic and opportunistic microorganisms. Silver-coated nanoparticles of 20–25 nm size were the most effective among all the nanoparticles without significant cytotoxicity, suggesting their use as antimicrobial additives in the process of fabrication of ambulatory and nonambulatory medical devices.

© 2010 Elsevier Inc. All rights reserved.

**Key words:** Silver nanoparticles; Titanium nanoparticles; Antimicrobial activity; Nanoparticle toxicity; DNA damage

In recent years the application of nanoparticles in various fields has expanded considerably. Nanoparticles possess unique physicochemical characteristics, such as a high ratio of surface area to mass, high reactivity, and sizes in the range of nanometers (10<sup>-9</sup> m).<sup>1</sup> Nanoparticles have been successfully used in nanochemistry to enhance the immobilization and activity of catalysts,<sup>2</sup> in medical and pharmaceutical nanoengineering for delivery of therapeutic agents,<sup>3</sup> in chronic disease diagnostics,

and in sensors.<sup>4</sup> Nanoparticles have been also used in clothing and in the food industry to limit bacterial growth.<sup>5,6</sup>

The continuing appearance of antibiotic resistance in pathogenic and opportunistic microorganisms obliges the scientific community to constantly develop new drugs and drug targets. Few new antibiotics have been introduced by the pharmaceutical industry in the last decade, and none of them have improved the activity against multidrug-resistant bacteria.<sup>7</sup> Because nanoparticles have demonstrated antimicrobial activities, the development of novel applications in this field makes them an attractive alternative to antibiotics. For instance, nanoparticles have been examined for their ability to reduce microbial infections in skin<sup>8</sup> and burn wounds,<sup>9</sup> and also to prevent bacterial colonization on various surface devices such as catheters<sup>10</sup> and prostheses.<sup>11</sup> Silver has been used extensively in topical preparations and to saturate bandages so as to restrict

Funding for this studies at Y.A.'s laboratory was provided by the TB Veterans Charitable Foundation and Enox Biopharma Inc. Comet experiments were supported by the Canadian Cancer Society (P.L.O.).

\*Corresponding author: Department of Medicine, Division of Infectious Diseases, University of British Columbia, 2733 Heather Street, Vancouver, British Columbia, Canada V5Z 3J5.

E-mail address: [hbach@interchange.ubc.ca](mailto:hbach@interchange.ubc.ca) (H. Bach).

1549-9634/\$ – see front matter © 2010 Elsevier Inc. All rights reserved.  
doi:10.1016/j.nano.2010.02.001

Table 1  
Crystal structure characteristics of TiO<sub>2</sub> particles used in this work

Nanoparticle	Anatase (%)	Rutile (%)
Ti-Pure R-902 (Ti <sup>1</sup> )	–	100
Zeta potential –27 mV		
Degussa P25 (Ti <sup>2</sup> )	75	25
Zeta potential –31 mV		
Parameters:		
Cell dimensions (Å)		
<i>a</i>	3.793	4.594
<i>c</i>	9.51	2.958
Number of molecules per cell		
Z value	4	2
Volume (Å <sup>3</sup> )	136.82	62.43
Density (g/cm <sup>3</sup> )	3.88	4.25

bacterial growth in injured skin.<sup>12,13</sup> Although the antimicrobial effects of silver derivatives are well documented, the mechanisms by which it exerts its bioactivity are not known. Some reports have proposed the formation and deposition of silver-sulfur granules on the microbial cell wall,<sup>14</sup> whereas other reports attribute its toxic effect to the inactivation of essential enzymes by forming complexes with the catalytic sulfur of thiol groups in cysteine residues.<sup>15,16</sup>

Although most of the studies are focused on nanoparticle applications, studies describing the impact of nanoparticles on human health are limited.<sup>17–19</sup> For instance, toxic effects of silver nanoparticles have been reported in mammalian cells, including alteration of the normal function of mitochondria, the increase of membrane permeability, and the generation of reactive oxygen species.<sup>20,21</sup>

In this work we report the synthesis of 15 nanoparticles with different physicochemical characteristics and sizes. We assessed their antimicrobial activities using a panel of bacterial and fungal pathogenic and opportunistic strains, and evaluated their cytotoxic effects by DNA damage and cell survival assays using a human-derived monocyte cell line.

## Methods

### Reagents

Titanium dioxide (TiO<sub>2</sub>) particles were purchased from Ti-Pure R-902 (Dupont, Wilmington, Delaware) and Degussa P25 (Degussa, Parsippany, New Jersey) (Table 1). Silver nitrate (AgNO<sub>3</sub>), sodium borohydride (NaBH<sub>4</sub>), gallic acid, and ammonium hydroxide (NH<sub>4</sub>OH) 30% (wt/wt) aqueous solution were purchased from Sigma-Aldrich (St Louis, Missouri).

### Synthesis and characterization of metallic nanoparticles

Nanoparticles used in this work were synthesized as follows.

#### 20- to 25-nm silver nanoparticles

A total of 100 mL of 0.001 M AgNO<sub>3</sub> was placed in a 250-mL reaction vessel. Under magnetic stirring, 10 mL of deionized water containing 0.01 g of gallic acid were added to the AgNO<sub>3</sub> solution. The pH of the solution was immediately adjusted to 11 using 1.0 M sodium hydroxide (NaOH).

#### 80- to 90-nm silver nanoparticles

A total of 100 mL of 0.001 M AgNO<sub>3</sub> prepared in deionized water was placed in a 250-mL reaction vessel inside an ultraviolet (UV) light reactor. Under magnetic stirring, 0.01 g of gallic acid in 10 mL of deionized water was added to the AgNO<sub>3</sub> solution, and the mixture was irradiated with UV light (254 nm, 15 W) for 30 minutes.

#### TiO<sub>2</sub>-Ag nanoparticles

The purchased TiO<sub>2</sub> particles were filtered, and dried. Hereafter, Ti-Pure R-902 particles were named Ti<sup>1</sup>, and Degussa P25 particles were named Ti<sup>2</sup>. These nanoparticles served as the basic units to synthesize three different nanoparticles with TiO<sub>2</sub>/Ag molar ratios of 10:1, 25:1, and 50:1. Nanoparticles were synthesized as follows: 0.2 g (2.5 mmol) of Ti<sup>1</sup> or Ti<sup>2</sup> particles were dispersed by ultrasound in 100 mL deionized water for 5 minutes. Immediately afterward, the 10:1, 25:1, and 50:1 molar ratios were obtained by adding 0.0425 g (0.25 mmol), 0.0169 g (0.1 mmol), or 0.00845 g (0.05 mmol) of AgNO<sub>3</sub>. The solution was magnetically stirred for about 30 minutes at pH 7, and then, 0.1 mmol or 0.25 mmol NaBH<sub>4</sub> (reducing agent), previously dissolved in 10 mL of deionized water, was added. The pH of the reaction was adjusted to 10 by adding NH<sub>4</sub>OH and magnetically stirring for another 30 minutes. In the nanoparticles synthesis using UV light as an activating agent, the procedure was as follows: 0.2 g (2.5 mmol) of Ti<sup>1</sup> or Ti<sup>2</sup> particles were dispersed by ultrasound in 100 mL deionized water for 5 minutes. Immediately afterwards, the 10:1, 25:1, and 50:1 molar ratios were obtained by adding 0.0425 g (0.25 mmol), 0.0169 g (0.1 mmol), or 0.00845 g (0.05 mmol) of AgNO<sub>3</sub>. The solution was magnetically stirred for about 30 minutes at pH 7 inside a UV reactor with UV lamps of wavelength 354 nm. Afterwards, the pH of the reaction was adjusted to 9–10 by adding NH<sub>4</sub>OH, and then, UV lamps were turned on and the solution was magnetically stirred for another 30 minutes. The conditions used in this preparation were carefully selected to control the size and the distribution of nanoparticles.<sup>22</sup> The vigorous chemical reduction yielded a brownish dispersion, and the particles obtained were filtered, washed, and dried for further characterization.

#### Nanoparticle characterization

Synthesized nanoparticles were characterized by UV-visible spectroscopy using an S2000 UV-Vis spectrophotometer from OceanOptics Inc. (Dunedin, Florida) Zeta potential measurements were carried out in ultrasonicated dispersions of 0.001 g nanoparticles in a 100 mL solution of sodium nitrate (1 mM) at room temperature (22–24°C). The pH of the dispersion was adjusted with either NaOH or nitric acid to obtain the desired pH value, which ranged between 2 and 11. Dynamic light scattering analysis was performed in a Malvern Zetasizer Nano ZS (Malvern Instruments, Worcestershire, United Kingdom) (Figure 1) operating with a He-Ne laser at a wavelength of 633 nm, and at a detection angle of 90 degrees. Samples were analyzed during 60 seconds at 25°C. Transmission electron microscopy analysis was performed on a JEOL JEM-1230 (JEOL, Tokyo, Japan) at an accelerating voltage of 100 kV. X-ray diffraction patterns were recorded with a GBC-Difftch MMA diffractometer

(Dandenong, Australia). The nickel-filtered CuK $\alpha$  ( $k = 1.54 \text{ \AA}$ ) radiation was used at 34.2 mA and 35 kV. All the characterization analyses except x-ray diffraction were made using the obtained aqueous dispersions of silver nanoparticles.

#### Microbial strains and culture media

The following gram-negative microorganisms were evaluated: *Escherichia coli* (ATCC 25922), *Acinetobacter baumannii* (ATCC BAA-747), and *Pseudomonas aeruginosa* (ATCC 27853). Among gram-positive microorganisms, *Bacillus subtilis* (ATCC 6633), *Mycobacterium smegmatis* (ATCC 700084), *Mycobacterium bovis* BCG (ATCC 35374), *Staphylococcus aureus* (ATCC 25923), and *S. aureus* methicillin-resistant (MRSA) (ATCC 700698) were assayed. *Candida albicans* (ATCC 14053), *Cryptococcus neoformans* (donated by Dr. James Kronstad, Michael Smith Laboratories, University of British Columbia, Vancouver, BC, Canada), and *Aspergillus niger* (ATCC 32656) were used as representatives of fungi. All organisms were grown in brain heart infusion broth (BD Biosciences, San Jose, California) with the exception of *M. smegmatis* and fungi, which were grown in Middlebrook 7H9 (BD Biosciences) supplemented with 10% OADC (BD Biosciences) and Sabouraud (BD Biosciences) Dextrose broths, respectively. Solid medium was obtained by adding 1.5% (wt/vol) agar.

#### Antimicrobial test

The microdilution method for estimation of minimum inhibitory concentration (MIC) values was carried out to evaluate the antimicrobial activity. The MIC values were determined on 96-well microdilution plates and according to published protocols.<sup>23,24</sup>

MICs were determined by incubating the organisms in 96-well microplates for 24 hours at 37°C with the exception of fungi, which were cultured at 28°C. *M. bovis* strain BCG, a slow-growing strain, was cultured on sealed plates (to avoid dehydration) at 37°C for 3 weeks, whereas *M. smegmatis*, a fast-growing strain, was cultured at 37°C for 48 hours. Microorganisms were exposed to serial dilutions of the nanoparticles, and the end points were determined when no turbidity in the well was observed. The antibacterial activities of the nanoparticles were compared to gentamicin, amikacin, and rifampicin, and amphotericin B was used as positive control for fungi. The turbidity background showed by nanoparticles was subtracted from the final reading. All assays were carried out in triplicate.

#### Measurement of nanoparticle cytotoxicity

Monocytic cell line THP-1 (ATCC 202) was cultured in RPMI 1640 (Hyclone, Logan, Utah) supplemented with 5% fetal calf serum (Hyclone), and 2 mM L-glutamine (StemCell Technologies, Vancouver British Columbia, Canada). Cells were dispensed in 96-well microplates at a density of  $3 \times 10^5$

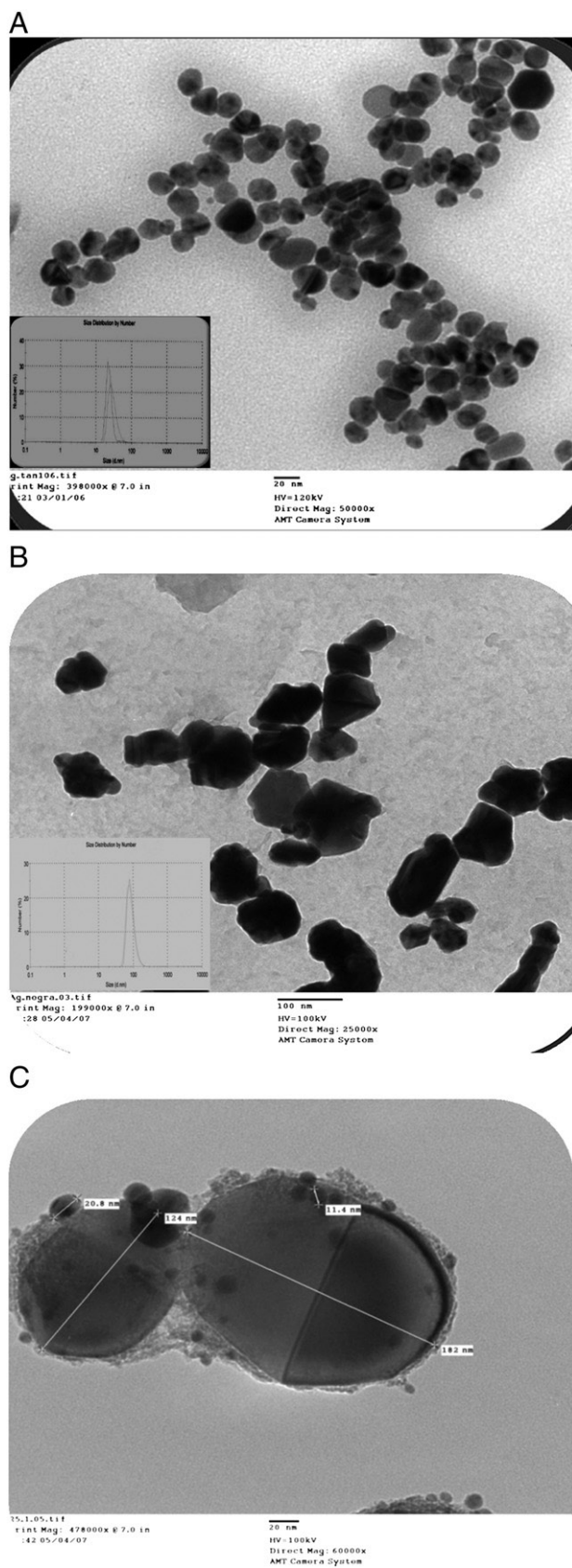


Figure 1. Characteristics of selected nanoparticles used in this work. Transmission electron micrographs of the composites synthesized. (A) Silver nanoparticles no. 1 (20–25 nm); (B) silver nanoparticles no. 15 (80–90 nm); (C) TiO<sub>2</sub>-Ag nanoparticles no. 9 (250–300 nm). Insets: distribution of the nanoparticles according to size using dynamic light scattering.



cells per well. Ten different concentrations were tested for each nanoparticle, in a final volume of 200  $\mu\text{L}$ /well. Microplates were incubated at 37°C in a humidified atmosphere supplemented with 5%  $\text{CO}_2$  for 24 hours. THP-1 cells treated for 6 hours with 5% hydrogen peroxide were used as positive controls, and untreated cells were used as negative control. The toxicity of the nanoparticles was measured by staining the monocytes with propidium iodide (PI) (Sigma-Aldrich) and according to published protocols.<sup>25</sup> The viability of the cells was assayed by Trypan blue (Sigma-Aldrich) staining, and cells were used only when a viable population of at least 95% was measured. PI emission was detected at 610–625 nm using the FL3 gate of a BD FACS Vantage SE Turbo sort cell sorter (BD, Mississauga, Ontario, Canada).

The effectiveness of the nanoparticles was expressed as the therapeutic index (TI), which is defined as the amount of a therapeutic agent that causes a therapeutic effect of 50% in the population. The TI estimates the extent to which the administration of a drug is safe, and it is calculated as  $\text{TI} = \text{LD}_{50}/\text{MIC}$ , where  $\text{LD}_{50}$  is the median lethal dose at which 50% of the cells die.<sup>26</sup> In this work we used the THP-1 toxicity as the values for  $\text{LD}_{50}$ , and the MICs for each microorganism.

#### Alkaline comet assay

DNA single-strand breaks and alkali-labile lesions were detected using the alkaline comet assay.<sup>27</sup> THP-1 monocyte cells were treated for 24 hours with the nanoparticles no. 1 and no. 10. Samples of untreated cells and positive controls consisting of cells exposed to 8-Gy x-rays were included in the experiment. Single cells were embedded in low-temperature-gelling agarose and pipetted onto an agarose-coated microscope slide. After 1 hour, cells were lysed using 0.26 M NaOH, 1.2 M sodium chloride, 0.1% *N*-lauroylsarcosine, and 100 mM EDTA. Cells were washed by rinsing the slides with an alkaline solution (0.03 M NaOH, 2 mM EDTA, pH 12.3) and subjected to alkaline gel electrophoresis using the same alkaline solution as the running buffer. Resulting comets were stained with 2.5  $\mu\text{g}/\text{mL}$  PI and analyzed by epifluorescence according to published protocols.<sup>8</sup> For each sample, 50 comets were analyzed on average.

## Results

#### Characteristics of nanoparticles

A total of 15 different nanoparticle types were studied: 2 prepared from silver (no. 1 and no. 2), 1 from  $\text{TiO}_2$  (no. 3), and 12 from a mixture of both silver and  $\text{TiO}_2$  using a combination of different molar ratios. The sizes of the nanoparticles were determined and varied between 20 and 300 nm (Table 2 and Figure 1).

#### Antimicrobial activities

To assess the antimicrobial activities of the nanoparticles synthesized in this work, a panel of selected strains of microorganisms was assayed, comprising both pathogens and opportunistic pathogens frequently encountered colonizing medical devices. The panel included gram-positive, gram-

Table 2  
Characteristics of the nanoparticles used in this work

Nanoparticles no.	Nanoparticle composition*	Molar ratio ( $\text{TiO}_2/\text{Ag}$ )	Size (nm)	Concentration ( $\mu\text{g}/\text{mL}$ )	
				$\text{TiO}_2$	Ag
1	Ag	–	20–25	–	107.8
2	Ag	–	80–90	–	107.8
3	$\text{TiO}_2$	–	250–300	400	–
4	$\text{Ti}^1\text{-Ag NaBH}_4$	10:1	250–300	90.00	10
5	$\text{Ti}^1\text{-Ag UV}$	10:1	300	90.00	10
6	$\text{Ti}^1\text{-Ag NaBH}_4$	25:1	250–300	99.50	0.5
7	$\text{Ti}^1\text{-Ag UV}$	25:1	250–300	99.50	0.5
8	$\text{Ti}^1\text{-Ag NaBH}_4$	50:1	250–300	99.65	0.35
9	$\text{Ti}^1\text{-Ag UV}$	50:1	250–300	99.65	0.35
10	$\text{Ti}^2\text{-Ag NaBH}_4$	10:1	250–300	90.00	10
11	$\text{Ti}^2\text{-Ag UV}$	10:1	250–300	90.00	10
12	$\text{Ti}^2\text{-Ag NaBH}_4$	25:1	250–300	99.50	0.5
13	$\text{Ti}^2\text{-Ag UV}$	25:1	250–300	99.50	0.5
14	$\text{Ti}^2\text{-Ag NaBH}_4$	50:1	250–300	99.65	0.35
15	$\text{Ti}^2\text{-Ag UV}$	50:1	250–300	99.65	0.35

\*  $\text{NaBH}_4$ ,  $\text{NaBH}_4$  used as reducing agent; UV, UV light used as activating agent.

negative, and fungal strains. Only nanoparticles that showed significant antimicrobial activities are displayed in Table 3. The silver nanoparticles no. 1 with a size of 20–25 nm showed the highest activity among all the nanoparticles tested (Table 3), with MIC averages ranging between 0.4–1.7  $\mu\text{g}/\text{mL}$  and 3–25  $\mu\text{g}/\text{mL}$  when bacterial and fungal strains, respectively, were tested (Figure 2). When the  $\text{TiO}_2$  nanoparticles were tested against bacterial strains alone or combined with silver, no significant activities were observed when compared to the silver nanoparticles no. 1 (data not shown). The activity of the silver nanoparticles no. 1 showed MICs comparable to those achieved with commercial antibiotics. For example, MICs of 0.53, 0.37, and 0.74  $\mu\text{g}/\text{mL}$  were measured when the silver nanoparticles no. 1 were tested against *E. coli*, *P. aeruginosa*, and *S. aureus*, whereas MICs of 0.83, 1.33, and 0.42  $\mu\text{g}/\text{mL}$  were recorded for gentamicin, respectively (Table 3). In addition, the combined  $\text{TiO}_2$  and silver nanoparticles (no. 10 and no. 15) showed a significant activity specific to fungal strains and ranged between 3 and 25  $\mu\text{g}/\text{mL}$ . For example, *C. albicans* showed a MIC of 6  $\mu\text{g}/\text{mL}$  when the silver nanoparticles no. 1 were assayed, performing better than fluconazole (64  $\mu\text{g}/\text{mL}$ ), and similar to amphotericin B (0.25  $\mu\text{g}/\text{mL}$ ) (Figure 3 and Table 3). The silver nanoparticles no. 1 also showed high activity against *M. smegmatis*, with a MIC of 0.46  $\mu\text{g}/\text{mL}$  compared to 0.85  $\mu\text{g}/\text{mL}$  of rifampicin (Figure 4 and Table 3).

#### Cytotoxicity and $\text{LD}_{50}$ calculation

THP-1 monocytes were used to determine the cytotoxic effects of nanoparticles. Ten different concentrations of the nanoparticles no. 1, no. 10, and no. 15 were assayed at 37°C for 24 hours using flow cytometry. The toxic effect of the nanoparticles no. 1 was dose-dependent as measured by the death rate of monocytes. Concentrations <2  $\mu\text{g}/\text{mL}$  showed no significant toxicity as less than a 20% death rate of monocytes

Table 3  
Minimum inhibitory concentrations ( $\mu\text{g/mL} \pm \text{SD}$ ) of nanoparticles showing antimicrobial activities

Nanoparticle no.	Gram positive					Gram negative			Fungi		
	BS	MB	MS	MRSA	SA	AB	EC	PA	AN	CA	CN
1	1.7 $\pm$ 0.2	1.1 $\pm$ 0.0	0.5 $\pm$ 0.3	0.5 $\pm$ 0.2	0.7 $\pm$ 0.2	0.4 $\pm$ 0.1	0.5 $\pm$ 0.2	0.4 $\pm$ 0.1	25 $\pm$ 0.0	6 $\pm$ 0.4	3 $\pm$ 0.0
10	86 $\pm$ 46	ND	>100	>100	>100	>100	>100	>100	25 $\pm$ 0.0	12.5 $\pm$ 0.0	12.5 $\pm$ 0.0
15	54 $\pm$ 0.0	11 $\pm$ 0.0	5 $\pm$ 2.4	54 $\pm$ 0.0	54 $\pm$ 0.0	20 $\pm$ 9.5	5.9 $\pm$ 0.5	20 $\pm$ 9.5	12.5 $\pm$ 0.0	6 $\pm$ 0.4	3.1 $\pm$ 0.0
PC	32 (G)	0.5 (R)	0.85 (R)	64 (G)	1 (G)	0.06 (Ak)	0.5 (Ak)	1 (Ak)	2 (A)	0.2 (A)	2 (A)

Gram-positive organisms: BS, *B. subtilis*; MB, *M. bovis*; MS, *M. smegmatis*; MRSA, methicillin-resistant *S. aureus*; SA, *S. aureus*.

Gram-negative: AB, *A. baumannii*; EC, *E. coli*; PA, *P. aeruginosa*.

Fungi: AN, *A. niger*; CA, *C. albicans*; CN, *C. neoformans*.

PC, positive control; ND, not determined; R, rifampicin; G, gentamicin; Ak, amikacin; A, amphotericin.

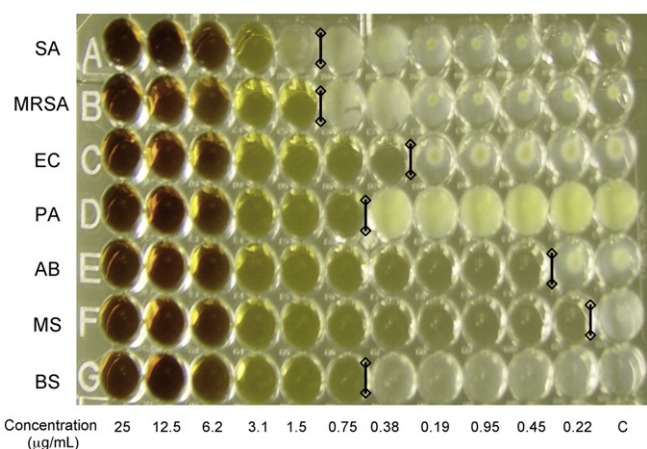


Figure 2. MICs of nanoparticles against bacterial strains. Serial dilutions of nanoparticles no. 1 were exposed to bacterial strains. Only nanoparticles no. 1 and selected bacterial strains are shown as an example of MIC determination. SA, *Staphylococcus aureus*; MRSA, methicillin-resistant *Staphylococcus aureus*; EC, *Escherichia coli*; PA, *Pseudomonas aeruginosa*; AB, *Acinetobacter baumannii*; MS, *Mycobacterium smegmatis*; BS, *Bacillus subtilis*. C, No nanoparticles added. Black bars denote the MICs for this specific experiment.

was observed (Figure 5). However, concentrations  $>5 \mu\text{g/mL}$  showed a significant increase in toxicity, reaching monocyte death rate of  $>50\%$ . In contrast, nanoparticles no. 10 and no. 15, showed a very slight toxicity showing a monocyte death rate varying between 15% and 25% even when the highest nanoparticle concentration (25  $\mu\text{g/mL}$ ) was assayed.

The cytotoxicity experiment allowed us to determine the  $\text{LD}_{50}$  of THP-1 cells exposed to the selected nanoparticles. Results showed that this parameter ranged between 10 and 367  $\mu\text{g/mL}$  (Table 4). Moreover, these results were used to calculate the TI of these nanoparticles, which measures the effectiveness of a compound. Results showed that the silver nanoparticles no. 1 possessed the highest TI calculated for bacterial strains (Table 4) but the lowest TI value for fungal strains.

#### Analysis of DNA damage using the alkaline comet assay

For the analysis of DNA damage we chose the nanoparticles no. 1, because they show significant activity when tested against

the assayed organisms, and the nanoparticles no. 10, because of their activity against fungal strains and their high  $\text{LD}_{50}$  and TI values. Results showed no evidence of the production of DNA single-strand breaks above the background level (Table 5) when THP-1 cells were exposed for 24 hours. The small reduction in tail moment and percentage of DNA in the comet tail was a result of a decrease in the percentage of S-phase cells that exhibit breaks at replication forks (Figure 5). Therefore, at doses that are bactericidal or fungicidal, there was no evidence that nanoparticles produced DNA damage in mammalian cells.

#### Discussion

In this work we report the synthesis and characterization of 15 types of nanoparticles using silver,  $\text{TiO}_2$ , or a combination of both compounds. We assayed these nanoparticles against a panel of opportunistic and pathogenic bacteria and fungal strains. We focused especially on those commonly associated with medical devices such as catheters and prostheses. Our results showed that the silver nanoparticles of 20–25 nm (nanoparticles no. 1) possess the highest antibacterial activity among all of the nanoparticles assayed. These nanoparticles have MICs ranging from 0.4 to 1.7  $\mu\text{g/mL}$  and are comparable to the MICs of commercial antibiotics. These nanoparticles exhibited limited antifungal activity, with the exception of *C. neoformans*, which was killed by them at MICs of 3 and 3.1  $\mu\text{g/mL}$  for the nanoparticles no. 1 and no. 15, respectively.  $\text{TiO}_2$  nanoparticles showed limited antifungal activity. However, when they were conjugated to silver under specific conditions during their synthesis, increased antifungal activity was observed. The synthesis conditions that facilitated antifungal activity included exposure of the  $\text{TiO}_2$  to either  $\text{NaBH}_4$  or UV light, in a molar ratio of 50:1 ( $\text{TiO}_2/\text{Ag}$ ). It is noteworthy that these antimicrobial activities were observed only with the  $\text{TiO}_2$  nanoparticles from Degussa ( $\text{Ti}^2$ ) and not from Ti-Pure R-902 ( $\text{Ti}^1$ ). The difference observed in the bioactivity between both  $\text{TiO}_2$  particles may be explained by their mineral composition. Although both particles show similar crystal structures of octahedrons,  $\text{Ti}^1$  is prepared from the mineral form of titanium  $\text{TiO}_2$ , rutile, whereas  $\text{Ti}^2$  contains another mineral form of  $\text{TiO}_2$  termed anatase (manufacturer's technical information). Although we are not able to determine the exact reason for the difference observed in their

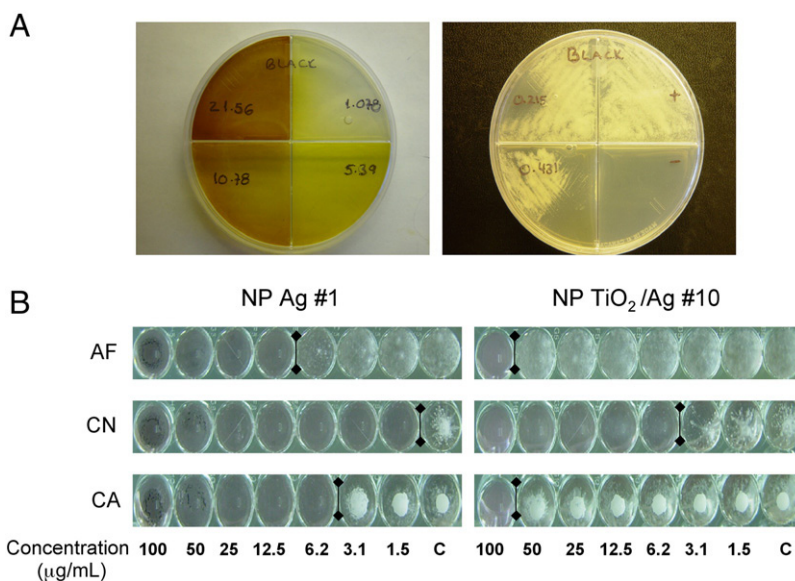


Figure 3. MICs of nanoparticles against *Mycobacterium bovis* and fungal strains. **(A)** Serial dilutions of nanoparticles no. 1 were exposed to *M. bovis* strain BCG. Numbers indicate the concentration of the nanoparticles ( $\mu\text{g/mL}$ ) spread on each quarter of the plate. +, No nanoparticles added; –, no bacteria added. **(B)** Serial dilutions of nanoparticles no. 1 and no. 10 exposed to fungal strains, and shown as an example. AF, *Aspergillus fumigatus*; CN, *Cryptococcus neoformans*; CA, *Candida albicans*. C, No nanoparticles added. NP, nanoparticle. Black bars denote the MIC for this specific experiment.

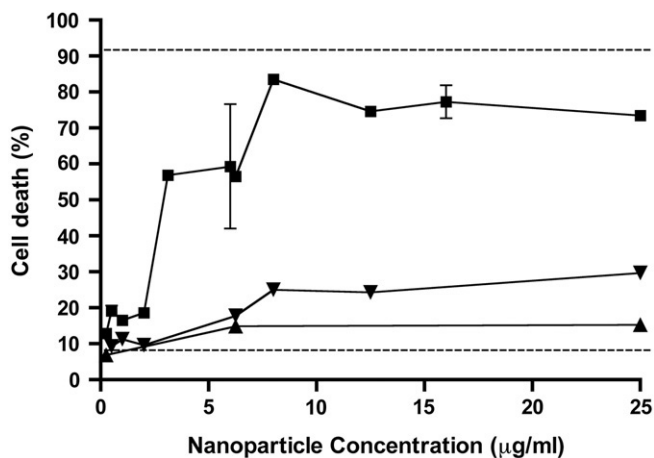


Figure 4. Cytotoxic effects of nanoparticles on THP-1 cells. Determination of the cytotoxic effects of nanoparticles no. 1 (squares), no. 10 (triangles), and no. 15 (inverted triangles) on THP-1 cells. Dashed lines represent treatment with 5% H<sub>2</sub>O<sub>2</sub> (upper line) (positive control), and no treatment (lower line) (negative control). Shown is the mean  $\pm$  SD of three independent experiments.

antimicrobial activities, it may be related to the intrinsic crystal parameters of both mineral forms (Table 1).

We and others have found that the sizes of the silver nanoparticles play an important role in their antimicrobial activity.<sup>24,28,29</sup> For example, a higher antimicrobial activity was observed only in silver nanoparticles measuring 20–25 nm but not in those measuring 80–90 nm. Previous studies have shown that silver nanoparticles of 29 nm showed MICs of 13 and 17  $\mu\text{g/mL}$  against *E. coli* and *S. aureus*, respectively.<sup>30</sup> However, here

we report an approximately 25-fold increase in the activity against the same strains (0.5 and 0.7  $\mu\text{g/mL}$ , respectively) when the size of the nanoparticles was reduced to 20–25 nm (Table 3). This suggests that there is a close association between size and activity and is in agreement with previous reports.<sup>24,28,29</sup>

In our study we report more efficient antibacterial activities for silver nanoparticles with MICs in a range between 0.4 and 1.7  $\mu\text{g/mL}$ , whereas other reports have shown lower antibacterial activities with MICs in a range between 1.69 and 13.5  $\mu\text{g/mL}$  using a similar broad spectrum of gram-negative and gram-positive strains, and a similar nanoparticle size, but prepared using maltose as a reducing agent.<sup>31</sup> Other groups have reported inferior antibacterial activities of silver nanoparticles using *E. coli* strains as a model. For instance, Thiel et al<sup>32</sup> reported that the synthesis of silver-doped titania nanoparticles using a sol-gel technique inhibited the growth of the nonpathogenic *E. coli* strain BL-21 at concentrations of 25.46  $\mu\text{g/cm}^2$ , whereas we reported a 100-fold increase in the antibacterial activity against the uropathogenic *E. coli* with an antibacterial effect of 0.24  $\mu\text{g/cm}^2$  as compared to the area of individual wells used in our experiments. Zhang and Chen<sup>33</sup> reported that concentrations greater than 2.4  $\mu\text{g/mL}$  suppressed the growth of *E. coli* using a silver nanocomposite powder [Ag (7.4 wt%)/TiO<sub>2</sub>], whereas Sondi and Salopek-Sondi reported a bacterial inhibition of 70% using a concentration of 10  $\mu\text{g/mL}$  nanoparticles (~12 nm).<sup>18</sup> Interestingly, Lok et al<sup>28</sup> reported a slightly superior antibacterial activity (3  $\mu\text{M}$  as compared to a calculated 4.6  $\mu\text{M}$  in our study) using smaller nanoparticles (~9 nm) but testing an *E. coli* strain isolated after selection against increasing concentrations of AgNO<sub>3</sub>.

According to the results reported here, the nanoparticles no. 1 showed promising results as an antimicrobial agent against



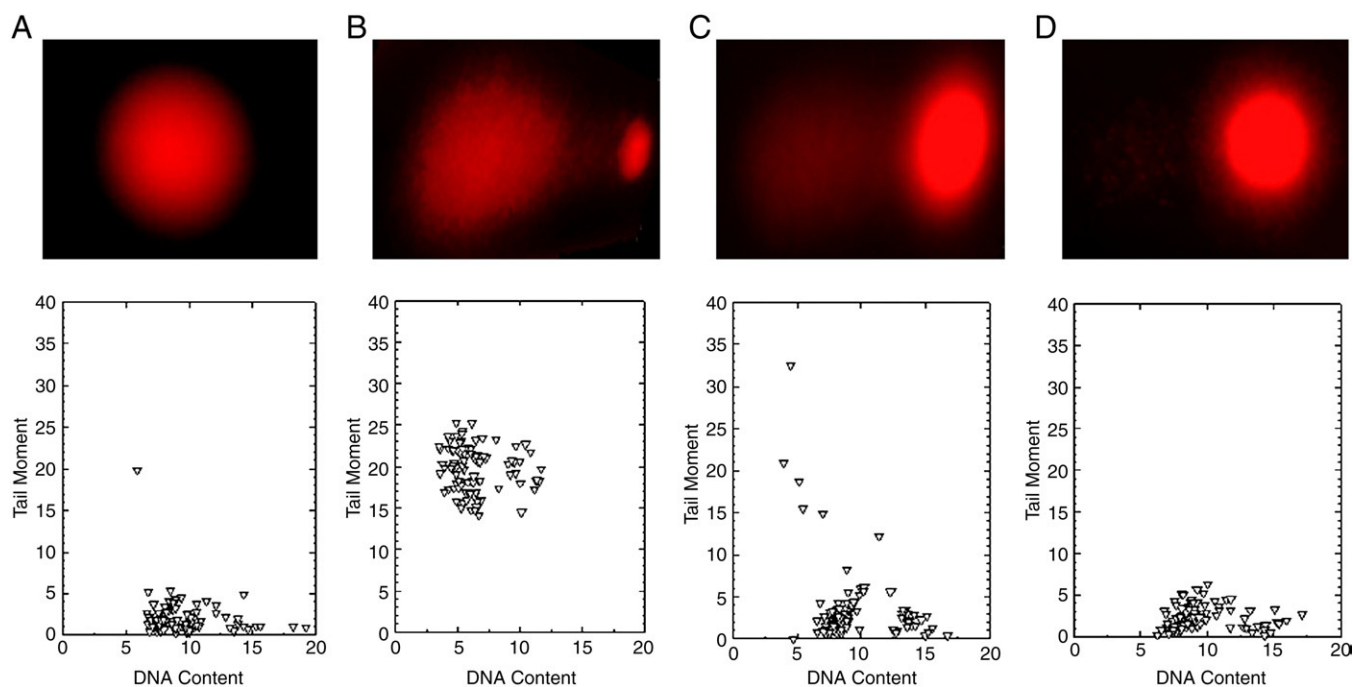


Figure 5. Detection of DNA damage on THP-1 cells exposed to nanoparticles. THP-1 cells were examined using alkali method. Shown are results from (A) negative control, (B) after 8-Gy x-ray exposure (positive control), (C) high concentration of nanoparticles no. 1, and (D) low concentration of nanoparticles no. 1.

Table 4  
Median lethal dose (LD<sub>50</sub>) and therapeutic index values

Nanoparticle no.	LD <sub>50</sub> ± SD (μg/mL)	Therapeutic index ± SD		
		Gram positive	Gram negative	Fungi
1	10 ± 3.4	13.86 ± 1.31	23.25 ± 0.63	0.9 ± 0.35
10	367.3 ± 13.1	2.6 ± 0.56	2.56 ± 0.32	22.1 ± 0.19
15	55.9 ± 0.4	1.57 ± 0.487	5.03 ± 0.68	10.7 ± 0.11

gram-positive and gram-negative bacteria. Noteworthy is its activity against the aggressive MRSA strain, and against *M. bovis*, suggesting that an alternative treatment against *M. tuberculosis* based on novel delivery systems may be developed. Although the antifungal activity was not as high as the antifungal used as references, more studies are necessary to test the possible application of these nanoparticles combined with other chemotherapies or nanoparticles with different composition.

We further analyzed the cytotoxic effect of the reported nanoparticles on THP-1 cells and found that a significant increase in their cytotoxicity was observed at concentrations greater than 5 μg/mL (Figure 4). Our findings are in agreement with other research groups, which showed that silver nanoparticles are cytotoxic in murine macrophages<sup>19</sup> and in fibroblasts<sup>17</sup> at concentrations of 10 and 50 μg/mL, respectively. We extended the studies of the cytotoxic effects of our nanoparticles by measuring the DNA damage in THP-1 cells using a comet assay. Results obtained from this experiment showed that no DNA

Table 5  
Data collection of comet assay using THP-1 cells

	THP-1 Cells			
	Negative control	Positive control (8 Gy)	Nanoparticles no. 1 (3.5 μg/mL)	Nanoparticles no. 10 (8 μg/mL)
DNA content	9.44 ± 2.54	6.34 ± 2.04	9.8 ± 3.24	9.33 ± 2.68
Tail moment	2.08 ± 2.20	19.6 ± 2.78	2.23 ± 1.37	3.29 ± 4.44
Percentage in tail	18.4 ± 11.4	76.6 ± 4.98	19.3 ± 10.9	23.1 ± 17.0
Tail length (mm)	18.7 ± 5.94	26.9 ± 4.14	18.7 ± 6.05	19.4 ± 5.71

damage was observed upon exposure of nanoparticles to THP-1 cells (Figure 5).

In conclusion, the antimicrobial activity of the nanoparticles showed that the silver nanoparticles no. 1 (20–25 nm) have great potential to be used as antimicrobial agents against microorganisms. In this work we showed that with a decrease in the size of the silver nanoparticle from 29 nm to 20–25 nm, their antimicrobial activities increased considerably. For instance, the development of metallic nanoparticles covering the surfaces of ambulatory and other medical devices would provide an alternative means to decrease the microorganism colonization and device-associated infection, including ventilator-associated pneumonia, central venous catheter infections, and catheter-associated urinary tract infections.

## Acknowledgment

We thank Mary Ko for technical assistance.

## References

- Kim JS, Kuk E, Yu KN, Kim JH, Park SJ, Lee HJ, et al. Antimicrobial effects of silver nanoparticles. *Nanomed Nanotechnol Biol Med* 2007;3: 95-101.
- Wang P. Nanoscale biocatalyst systems. *Curr Opin Biotechnol* 2006; 17:574-9.
- Zhang L, Gu FX, Chan JM, Wang AZ, Langer RS, Farokhzad OC. Nanoparticles in medicine: therapeutic applications and developments. *Clin Pharmacol Ther* 2008;83:761-9.
- Hong B, Kai J, Ren Y, Han J, Zou Z, Ahn CH, et al. Highly sensitive rapid, reliable, and automatic cardiovascular disease diagnosis with nanoparticle fluorescence enhancer and MEMS. *Adv Exp Med Biol* 2008;614:265-73.
- Chau CF, Wu SH, Yen GC. The development of regulations for food nanotechnology. *Trends in Food Sci Technol* 2007;18:269-80.
- Vigneshwaran N, Kathe AA, Varadarajan PV, Nachane RP, Balasubramanya RH. Functional finishing of cotton fabrics using silver nanoparticles. *J Nanosci Nanotechnol* 2007;7:1893-7.
- Conlon JM, Kolodziejek J, Nowotny N. Antimicrobial peptides from ranid frogs: taxonomic and phylogenetic markers and a potential source of new therapeutic agents. *Biochim Biophys Acta* 2004;1696:1-14.
- Paddle-Ledinek JE, Nasa Z, Cleland HJ. Effect of different wound dressings on cell viability and proliferation. *Plastic Reconstruct Surg* 2006;117:110S-8S.
- Ulkur E, Oncul O, Karagoz H, Yeniz E, Celikoz B. Comparison of silver-coated dressing (Acticoat), chlorhexidine acetate 0.5% (Bactigrass), and fusidic acid 2% (Fucidin) for topical antibacterial effect in methicillin-resistant *Staphylococci*-contaminated, full-skin thickness rat burn wounds. *Burns* 2005;31:874-7.
- Samuel U, Guggenbichler JP. Prevention of catheter-related infections: the potential of a new nano-silver impregnated catheter. *Int J Antimicrob Agents* 2004;23(Suppl 1):S75-S78.
- Gosheger G, Harges J, Ahrens H, Streitburger A, Buerger H, Erren M, et al. Silver-coated megaendoprostheses in a rabbit model—an analysis of the infection rate and toxicological side effects. *Biomaterials* 2004;25: 5547-56.
- Nomiya K, Yoshizawa A, Tsukagoshi K, Kasuga NC, Hirakawa S, Watanabe J. Synthesis and structural characterization of silver(I), aluminium(III) and cobalt(II) complexes with 4-isopropyltropolone (hinokitiol) showing noteworthy biological activities. Action of silver (I)-oxygen bonding complexes on the antimicrobial activities. *J Inorg Biochem* 2004;98:46-60.
- Gupta A, Silver S. Silver as a biocide: will resistance become a problem? *Nat Biotechnol* 1998;16:888.
- Feng QL, Wu J, Chen GQ, Cui FZ, Kim TN, Kim JO. A mechanistic study of the antibacterial effect of silver ions on *Escherichia coli* and *Staphylococcus aureus*. *J Biomed Mater Res* 2000;52:662-8.
- Matsumura Y, Yoshikata K, Kunisaki S, Tsuchido T. Mode of bactericidal action of silver zeolite and its comparison with that of silver nitrate. *Appl Environ Microbiol* 2003;69:4278-81.
- Gupta A, Maynes M, Silver S. Effects of halides on plasmid-mediated silver resistance in *Escherichia coli*. *Appl Environ Microbiol* 1998;64: 5042-5.
- Hsin YH, Chen CF, Huang S, Shih TS, Lai PS, Chueh PJ. The apoptotic effect of nanosilver is mediated by a ROS- and JNK-dependent mechanism involving the mitochondrial pathway in NIH3T3 cells. *Toxicol Lett* 2008;179:130-9.
- Sondi I, Salopek-Sondi B. Silver nanoparticles as antimicrobial agent: a case study on *E. coli* as a model for Gram-negative bacteria. *J Colloid Interface Sci* 2004;275:177-82.
- Yen HJ, Hsu SH, Tsai CL. Cytotoxicity and immunological response of gold and silver nanoparticles of different sizes. *Small* 2009;5: 1553-61.
- Braydich-Stolle L, Hussain S, Schlager JJ, Hofmann MC. In vitro cytotoxicity of nanoparticles in mammalian germline stem cells. *Toxicol Sci* 2005;88:412-9.
- Hussain SM, Hess KL, Gearhart JM, Geiss KT, Schlager JJ. In vitro toxicity of nanoparticles in BRL 3A rat liver cells. *Toxicol in Vitro* 2005; 19:975-83.
- Niño-Martínez N, Martínez-Castañón GA, Aragón-Piña A, Martínez-Gutierrez F, Martínez-Mendoza JR, Ruiz F. Characterization of silver nanoparticles synthesized on titanium dioxide fine particles. *Nanotechnology* 2008;065711:19.
- Clinical and Laboratory Standards Institute. Reference method for broth dilution antifungal susceptibility testing of yeasts; third informational supplement. Wayne (Penn): CLSI; Approved standard M27-A; 1997.
- Clinical and Laboratory Standards Institute. Susceptibility testing of mycobacteria, nocardia, and other aerobic actinomycetes. Wayne (Penn): CLSI; 2003.
- Pick N, Cameron S, Arad D, Av-Gay Y. Screening of compounds toxicity against human monocytic cell line-THP-1 by flow cytometry. *Biol Proced Online* 2004;6:220-5.
- Casarett L, Klaassen CD, Doull J. In: Klaassen CD, editor. Casarett and Doull's toxicology: the basic science of poisons. New York: McGraw-Hill; 2001. p. 23-4.
- Olive PL, Banath JP, Durand RE. Heterogeneity in radiation-induced DNA damage and repair in tumor and normal cells measured using the "comet" assay. *Radiat Res* 1990;122:86-94.
- Lok CN, Ho CM, Chen R, He QY, Yu WY, Sun H, et al. Silver nanoparticles: partial oxidation and antibacterial activities. *J Biol Inorg Chem* 2007;12:527-34.
- Morones JR, Elechiguerra JL, Camacho A, Ramirez JT. The bactericidal effect of silver nanoparticles. *Nanotechnology* 2005;16: 2346-53.
- Martínez-Castañón GA, Niño-Martínez N, Martínez-Gutierrez F, Martínez-Mendoza JR, Ruiz F. Synthesis and antibacterial activity of silver nanoparticles with different sizes. *J Nanoparticle Res* 2008;10: 1343-8.
- Panacek A, Kvittek L, Prucek R, Kolar M, Vecerova R, Pizurova N, et al. Silver colloid nanoparticles: synthesis, characterization, and their antibacterial activity. *J Phys Chem* 2006;110:16248-53.
- Thiel J, Pakstis L, Buzby S, Raffi M, Ni C, Pochan DJ, et al. Antibacterial properties of silver-doped titania. *Small* 2007;3:799-803.
- Zhang H, Chen G. Potent antibacterial activities of Ag/TiO<sub>2</sub> nanocomposite powders synthesized by a one-pot sol-gel method. *Environ Sci Technol* 2009;43:2905-10.